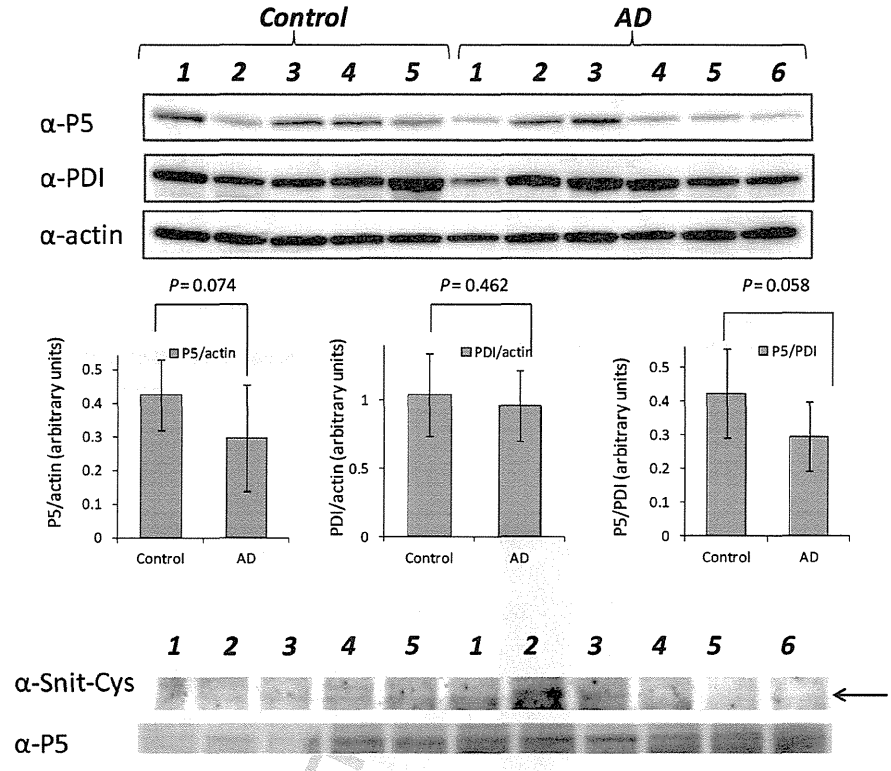

Fig. 3. Western blot analysis of P5 protein in human brain samples. A) Western blotting of PDI and P5 in human brain samples. Protein extracts from six patients with AD and five controls were analyzed by western blotting using anti-PDI and anti-P5 antibodies. β-actin was used as a loading control. Bands were visualized by chemiluminescence as described in the Materials and Methods. B) Expression levels of PDI and P5 in control and AD brain samples. Expression levels were calculated as described in the Materials and Methods. Data represent the mean ± SEM. C) S-nitrosylation of P5 protein in AD brain samples. P5 protein was immunoprecipitated with anti-P5 antibody using extracts obtained from brain samples, and then western blotting was performed using anti-SNO-Cys antibodies as described in the Materials and Methods. Arrow indicates the location of S-nitrosylated P5 protein.

depletion of Ca^{2+} in the ER (Fig. 4, lower graph). It is interesting that over-expression of PDI or P5 by transient transfection with expression vectors had no effect on the viability of SH-SY5Y cells under ER stress (data not shown). These results suggest that the appropriate expression level of P5 is significant for neuronal cell viability especially during ER stress, and these results are correlated with those of western blot analysis using patient samples as discussed above.

DISCUSSION

The ER is a target for endogenously generated reactive oxygen species during aging. It was previously reported that PDI and BiP were oxidatively modified within the livers of elderly mice [16]. Specific activity measurements, performed on purified protein samples obtained from young and old mouse livers, showed definite decreases in BiP ATPase activity and dramatic reductions in PDI enzymatic activity with age. Protein folding and other PDI- and BiP-mediated activities are diminished during aging. Furthermore, the relative loss of these chaperon-like activities could directly contribute to the age-dependent accumulation of misfolded proteins, which is a characteristic of the aging phenotype [16]. As age is the highest risk factor for AD, ER chaperon proteins may be decreased with age, allowing accumulation of misfolded proteins.

Deposition of Aβ is a major pathological hallmark of AD. Recent studies of amyloid-β protein precursor (AβPP) metabolism demonstrated a β/γ-secretase pathway located in the ER that leads to intracellular generation of soluble AβPP and $Aβ_{42}$ peptide [17]. Thus, the ER may be a key site of amyloidogenic AβPP metabolism and AD pathogenesis. Metabolic labeling and immunoprecipitation of transiently transfected human embryonic kidney 293

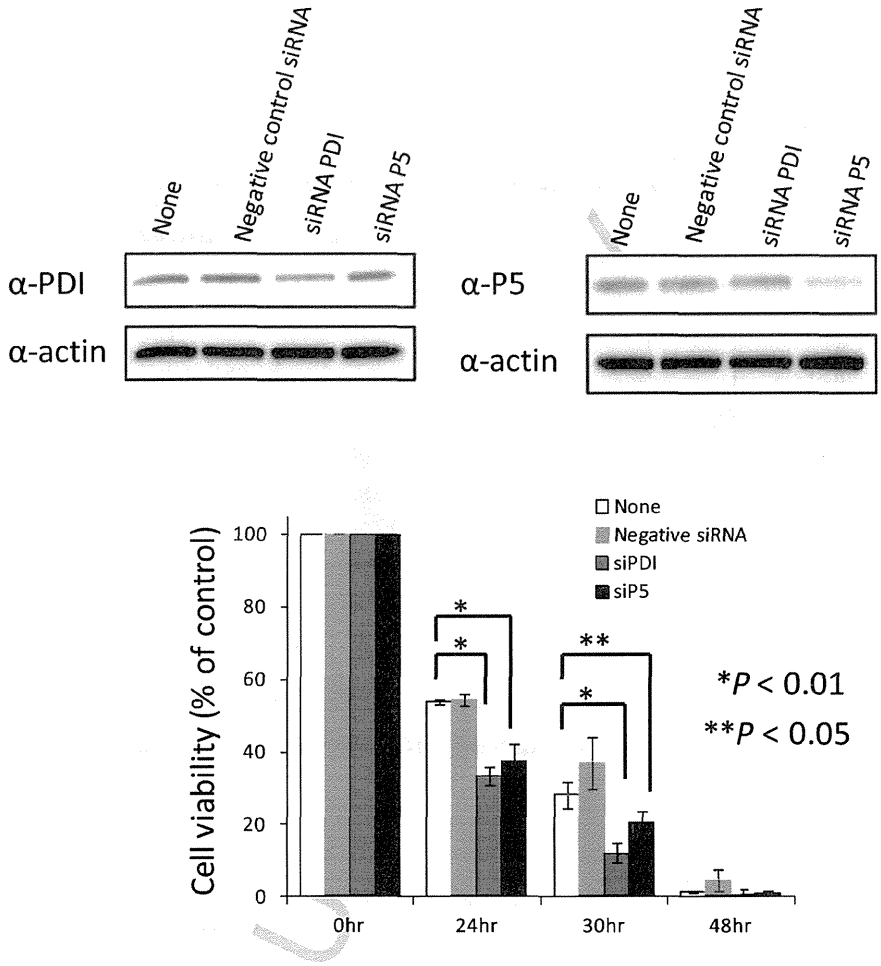

Fig. 4. Effect of knock-down of PDI or P5 on the viability of SH-SY5Y cells under ER stress. Using SH-SY5Y cells, the expression levels of PDI and P5 were confirmed by western blotting 48 h after siRNA transfection (upper panels). β-Actin was used as the loading control. The viability of SH-SY5Y cells after knock-down using siRNA for PDI or P5 with or without induction of ER stress by thapsigargin was assayed as described in the Materials and Methods (lower graph). Cell viability (none, negative siRNA, siPDI, and siP5) without the induction of ER stress at each time (0 h, 24 h, 30 h, and 48 h) was set as a control (i.e., 100%). Data represent the mean ± SD from experiments performed in triplicate. $*p < 0.01$, $**p < 0.05$.

cells demonstrated co-precipitation of AβPP with BiP, revealing their transient interaction in the ER [17]. Maturation of cellular AβPP was impaired by this interaction. It was previously reported that the protein level of BiP was increased in the temporal cortex and hippocampus of AD brain as determined by western blot analysis and, in particular, the protein level of BiP was increased in Braak stages B and C for amyloid deposits [18]. On the other hand, it was also reported that P5 formed a complex with BiP, and that P5 was a specific substrate protein for BiP [19]. In the present study, we found that the protein levels of P5 were decreased in AD (Fig. 3A, B). It has previously been shown that BiP is not co-localized with NFTs in AD brain [11]; however, P5 was co-localized with NFTs in the present study. It is known that PDI prevents neurotoxicity associated with ER stress and protein misfolding, but NO can block the protective effect of the enzyme through S-nitrosylation [9]. This inhibition of PDI leads to ER stress, which can induce apoptosis. It was previously shown that PDI was S-nitrosylated but the level was not increased in AD [9, 15]. In the present study, we confirmed that the protein level of PDI was not up-regulated in AD (Fig. 3A, B). But the protein level of P5 was down-regulated in AD. The expression level may depend on the clinical stages. In addition, we observed S-nitrosylated P5 in two brains from patients with AD, but it was never found in

control brains. As P5 and PDI were S-nitrosylated in AD, S-nitrosylation of members of the PDI family may lead to loss of function. Recently, it was reported that PDI was also S-nitrosylated in amyotrophic lateral sclerosis [20]. Further investigation is needed to determine whether S-nitrosylation of PDI or P5 occurs in other neurodegenerative diseases.

In the present study, we demonstrated the presence of anti-P5 antibody-immunopositive NFTs. Furthermore, AT8-tau and P5 were co-localized in NFTs. To our knowledge, this is the first report of P5-immunopositive inclusion in AD. We assume that NO inhibited P5 and led to the accumulation of unfolded proteins in AD. Abnormally phosphorylated tau or other proteins may accumulate in NFTs and cause ER stress in AD. As P5 acts as a chaperon in neurons, it may bind to tau and become included in NFTs. The co-localization of P5 and tau in NFTs may be linked to the formation of these inclusions. In addition to degeneration of neurons, the cell structure is markedly changed in neurodegenerative disease. The ER is damaged and P5 may come out of the ER. In many destroyed proteins, P5 and tau may be binding strongly and then they are co-localized in NFTs. We also found that knock-down of P5 could decrease the viability of neuronal cells during ER stress induced by thapsigargin, compared with that of control cells. Taken together, these findings suggest that the role of P5 during ER stress is essential for neuronal cell viability, particularly among aging cells.

A limitation of our study is that the samples have serious variation due to the condition after mortal or clinical stages. Thus, we currently speculate that the level of P5 protein would be decreased depending on the clinical stages of AD, and this is one of the most intriguing issues which should make it clearer in our next study.

In summary, we have demonstrated the presence of P5-immunopositive NFTs in AD. Furthermore, we showed that S-nitrosylated P5 was present and the expression level of P5 was decreased in AD brains compared with that of control brains. We speculate that P5 may be increased in early stage due to ER stress. But ER stress was prolonged and then a lot of neuronal cells were destroyed. Finally, P5 may be decreased in advanced stage. In addition, we found that ER stress with P5 dysfunction can cause neuronal cell death. In AD, NO may inhibit P5 by inducing S-nitrosylation, which inhibits its enzymatic activity and thus allows protein misfolding to occur. The accumulation of misfolded proteins induces ER stress, which can cause apoptosis of neuronal cells. These results suggest that P5 could be a therapeutic target to prevent ER stress in neuronal cells in AD.

ACKNOWLEDGMENTS

We thank Mitsuko Tachi, Maiko Yamada, Keiko Shimoura (Department of Pharmacoepidemiology, Kyoto University), and Akiko Yoshida (Department of Neurology, Kyoto University) for excellent technical assistance. This work was in part supported by a research grant from the Alzheimer's Association (IIRG-09-132098) and CREST and Soshinkai Nagaokakyo Hospital.

Authors' disclosures available online (http://www.j-alz.com/disclosures/view.php?id=1889).

SUPPLEMENTARY MATERIAL

Supplementary figures are available in the electronic version of this article: http://dx.doi.org/10.3233/JAD-130632.

REFERENCES

[1] Morishima-Kawashima M, Ihara Y (2002) Alzheimer's disease: Beta-amyloid protein and tau. *J Neurosci Res* **70**, 392-401.

[2] Cras P, Kawai M, Lowery D, Gonzalez-DeWhitt P, Greenberg B, Perry G (1991) Senile plaque neurites in Alzheimer disease accumulate amyloid precursor protein. *Proc Natl Acad Sci U S A* **88**, 7552-7556.

[3] Nakamura T, Lipton SA (2009) Cell death: Protein misfolding and neurodegenerative diseases. *Apoptosis* **14**, 455-468.

[4] Colton CA, Wilcock DM, Wink DA, Davis J, Van Nostrand WE, Vitek MP (2008) The effects of NOS2 gene deletion on mice expressing mutated human AbetaPP. *J Alzheimers Dis* **15**, 571-587.

[5] Kimura T, Horibe T, Sakamoto C, Shitara Y, Fujiwara F, Komiya T, Yamamoto A, Hayano T, Takahashi N, Kikuchi M (2008) Evidence for mitochondrial localization of P5, a member of the protein disulphide isomerase family. *J Biochem* **144**, 187-196.

[6] Noiva R, Lennarz WJ (1992) Protein disulfide isomerase. A multifunctional protein resident in the lumen of the endoplasmic reticulum. *J Biol Chem* **267**, 3553-3556.

[7] Kimura T, Nishida A, Ohara N, Yamagishi D, Horibe T, Kikuchi M (2004) Functional analysis of the CXXC motif using phage antibodies that cross-react with protein disulphide-isomerase family proteins. *Biochem J* **382**, 169-176.

[8] Shitara Y, Tonohora Y, Goto T, YamadaY, Miki T, Makino H, Miwa M, Komiya T (2012) Mitochondrial P5, a member of protein disulphide isomerase family, suppresses oxidative stress-induced cell death. *J Biochem* **152**, 73-85.

[9] Uehara T, Nakamura T, Yao D, Shi ZQ, Gu Z, Ma Y, Masliah E, Nomura Y, Lipton SA (2006) S-nitrosylated protein-disulphide isomerase links protein misfolding to neurodegeneration. *Nature* **441**, 513-517.

[10] Honjo Y, Ito H, Horibe T, Takahashi R, Kawakami K (2010) Protein disulfide isomerase-immunopositive inclusions in patients with Alzheimer disease. *Brain Res* **1349**, 90-96.
[11] Hoozemans JJ, Veerhuis R, Van Haastert ES, Rozemuller JM, Baas F, Eikelenboom P, Scheper W (2005) The unfolded protein response is activated in Alzheimer's disease. *Acta Neuropathol* **110**, 165-172.
[12] Honjo Y, Ito H, Horibe T, Shimada H, Nakanishi A, Mori H, Takahashi R, Kawakami K (2012) Derlin-1-immunopositive inclusions in patients with Alzheimer's disease. *NeuroReport* **23**, 611-615.
[13] Kohno M, Horibe T, Haramoto M, Yano Y, Ohara K, Nakajima O, Matsuzaki K, Kawakami K (2011) A novel hybrid peptide targeting EGFR-expressing cancers. *Eur J Cancer* **47**, 773-783.
[14] Horibe T, Kohno M, Haramoto M, Ohara K, Kawakami K (2011) Designed hybrid TPR peptide targeting Hsp90 as a novel anticancer agent. *J Transl Med* **14**, 8.
[15] Kim HT, Russell RL, Raina AK, Harris PL, Siedlak SL, Zhu X, Petersen RB, Shimohama S, Smith MA, Perry G (2000) Protein disulfide isomerase in Alzheimer disease. *Antioxid Redox Signal* **2**, 485-489.
[16] Nuss JE, Choksi KB, DeFord JH, Papaconstantinou J (2008) Decreased enzyme activities of chaperones PDI and BiP in aged mouse livers. *Biochem Biophys Res Commun* **365**, 355-361.
[17] Yang Y, Turner RS, Gaut JR (1998) The chaperone BiP/GRP78 binds to amyloid precursor protein and decreases Abeta40 and Abeta42 secretion. *J Biol Chem* **273**, 25552-25555.
[18] Hoozemans JJ, Stieler J, van Haastert ES, Veerhuis R, Rozemuller AJ, Baas F, Eikelenboom P, Arendt T, Scheper W (2006) The unfolded protein response affects neuronal cell cycle protein expression: Implications for Alzheimer's disease pathogenesis. *Exp Gerontol* **41**, 380-386.
[19] Jessop CE, Watkins RH, Simmons JJ, Tasab M, Bulleid NJ (2009) Protein disulphide isomerase family members show distinct substrate specificity: P5 is targeted to BiP client proteins. *J Cell Sci* **122**, 4287-4295.
[20] Walker AK, Farg MA, Bye CR, McLean CA, Horne MK, Atkin JD (2010) Protein disulphide isomerase protects against protein aggregation and is S-nitrosylated in amyotrophic lateral sclerosis. *Brain* **133**, 105-116.

Acta Neuropathol (2014) 127:685–698
DOI 10.1007/s00401-014-1259-1

ORIGINAL PAPER

Neurofibrillary tangle formation by introducing wild-type human tau into APP transgenic mice

Tomohiro Umeda · Satomi Maekawa · Tetsuya Kimura · Akihiko Takashima · Takami Tomiyama · Hiroshi Mori

Received: 24 August 2013 / Revised: 6 February 2014 / Accepted: 6 February 2014 / Published online: 15 February 2014

Abstract Senile plaques comprised of Aβ aggregates and neurofibrillary tangles (NFTs) composed of hyperphosphorylated tau filaments are the hallmarks of Alzheimer's disease (AD). A number of amyloid precursor protein (APP) transgenic (Tg) mice harboring APP mutations have been generated as animal models of AD. These mice successfully display amyloid plaque formation and subsequent tau hyperphosphorylation, but seldom induce NFT formations. We have demonstrated that the APP_{OSK}-Tg mice, which possess the E693Δ (Osaka) mutation in APP and thereby accumulate Aβ oligomers without plaques, exhibit tau hyperphosphorylation at 8 months, but not NFT formation even at 24 months. We assumed that APP-Tg mice, including ours, failed to form NFTs because NFT formation requires human tau. To test this hypothesis, we crossbred APP_{OSK}-Tg mice with tau-Tg mice (tau264), which express low levels of 3-repeat and 4-repeat wild-type human tau without any pathology. The resultant double Tg mice displayed tau hyperphosphorylation at 6 months and NFT formation at 18 months in the absence of tau mutations. Importantly, these NFTs contained both 3-repeat and 4-repeat human tau, similar to those in AD. Furthermore, the double Tg mice exhibited Aβ oligomer accumulation, synapse loss, and memory impairment at 6 months and neuronal loss at 18 months, all of which appeared earlier than in the parent APP_{OSK}-Tg mice. These results suggest that Aβ and human tau synergistically interact to accelerate each other's pathology, that the presence of human tau is critical for NFT formation, and that Aβ oligomers can induce NFTs in the absence of amyloid plaques.

Keywords Aβ oligomers · Tau filaments · Synapse loss · Neuronal loss · Alzheimer's disease

Introduction

Senile plaques comprised of Aβ fibrils and neurofibrillary tangles (NFTs) composed of hyperphosphorylated tau filaments are the hallmarks of Alzheimer's disease (AD). It was believed that Aβ deposition triggers abnormal phosphorylation of tau, which leads to NFT formation and neurodegeneration [17]. Based on this hypothesis, a number of amyloid precursor protein (APP) transgenic (Tg) mice have been generated as animal models of AD. By introducing one or more APP mutations identified in familial AD into the transgene, these mice successfully displayed amyloid plaque formation and subsequent tau hyperphosphorylation within neurons surrounding the plaques, but seldom induced NFT formations [12]. Several groups have established mouse models of AD showing both amyloid plaques and NFTs by crossbreeding mutant APP-Tg mice with mutant tau-Tg mice [4, 18, 26, 35, 37, 38, 41]. However, these models do not exactly reflect the pathogenesis of AD,

Electronic supplementary material The online version of this article (doi:10.1007/s00401-014-1259-1) contains supplementary material, which is available to authorized users.

T. Umeda · S. Maekawa · T. Tomiyama (✉) · H. Mori
Department of Neuroscience, Osaka City University Graduate School of Medicine, 1-4-3 Asahimachi, Abeno-ku, Osaka 545-8585, Japan
e-mail: tomi@med.osaka-cu.ac.jp

T. Umeda · T. Tomiyama · H. Mori
Core Research for Evolutional Science and Technology, Japan Science and Technology Agency, Kawaguchi, Japan

T. Kimura · A. Takashima
Department of Aging Neurobiology, Center for Development of Advanced Medicine for Dementia, National Center for Geriatrics and Gerontology, Obu, Japan

since no mutations in tau have been found in AD and since tau mutations themselves can cause NFT formation in mice independent of Aβ deposition [14].

Recent evidence suggests that Aβ oligomers, rather than Aβ fibrils, are the causal molecule in AD [23]. In cultured rat primary neurons, exogenously added Aβ oligomers induced tau hyperphosphorylation and neurodegeneration [11, 21]. We have shown that the E693Δ (Osaka) mutation in APP, which was found in Japanese pedigrees with familial AD, causes disease by enhancing Aβ oligomerization without amyloid plaque formation [47]. We generated APP-Tg mice harboring this mutation (APP_{OSK}-Tg mice) to study the pathological roles of Aβ oligomers in AD in vivo [46]. The levels of expression of human APP in the mice were almost the same as those of endogenous mouse APP. The APP_{OSK}-Tg mice showed intraneuronal accumulation of Aβ oligomers, synapse loss, and memory impairment at 8 months and eventual neuronal loss at 24 months. Tau hyperphosphorylation also occurred at 8 months, but NFT formation did not even at 24 months. We assumed that APP-Tg mice, including ours, failed to form NFTs because these mice lacked certain factors necessary for NFT formation.

The formation of NFTs in old age has been reported to occur not only in humans but also in other species, including chimpanzees [39], baboons [40], cynomolgus monkeys [36], cheetahs [42], and cats [6]. On the other hand, mice and rats are known not to form NFTs. We compared the amino acid sequences of tau across humans, chimpanzees, cats, and mice, which are available from the NCBI database. We found apparent differences in amino acid sequence between human and mouse tau, particularly in the N-terminal regions. In contrast, chimpanzee tau is almost identical to human tau and cat tau shows higher structural homology with human tau than with mouse tau. These observations led us to hypothesize that NFT formation requires certain sequences which exist in human tau but not in mouse tau.

To elucidate this possibility, here we generated double Tg mice by crossbreeding APP_{OSK}-Tg mice with our wild-type human tau-Tg mice. The tau-Tg mice, originally referred to as line 264 and hereafter termed tau264, were designed to express both 3-repeat (3R) and 4-repeat (4R) human tau at a comparable ratio to that in adult human by inserting tau intronic sequences into both sides of tau exon 10 in the transgene [48]. The levels of expression of human tau in tau264 mice were only 10 % those of endogenous mouse tau, and no pathological changes were observed even at 24 months. The resultant double Tg mice displayed tau hyperphosphorylation at 6 months and NFT formation at 18 months in the absence of tau mutations. Importantly, these NFTs contained both 3R and 4R human tau, similar to those in AD [15]. Furthermore, double Tg mice exhibited intraneuronal accumulation of Aβ oligomers, synapse loss, and memory impairment at 6 months and neuronal loss at 18 months, all of which appeared earlier than in the parent APP_{OSK}-Tg mice. These results suggest that Aβ and human tau synergistically interact to accelerate each other's pathology and that the presence of human tau is critical for Aβ-induced NFT formation. Our findings also indicate that Aβ oligomers can induce NFTs in the absence of amyloid plaques.

Materials and methods

Generation of double Tg mice

Heterozygotes of the APP_{OSK}-Tg mice [46], which express human APP695 with the Osaka mutation under the mouse prion promoter, were mated with heterozygotes of the tau264 mice [48], which express 3R and 4R wild-type human tau by the presence of tau intronic sequences under the mouse calcium/calmodulin-dependent kinase IIα promoter. The siblings were examined for their genotype by genome PCR and were accordingly divided into four groups: non-Tg, APP_{OSK}-Tg, tau264, and double Tg expressing both APP_{OSK} and wild-type human tau. The single and double Tg mice were heterozygous for each transgene of interest and have the same genetic background as C57BL/6 mice. All animal experiments were approved by the ethics committee of Osaka City University (Osaka, Japan) and were performed in accordance with the Guide for Animal Experimentation, Osaka City University. Every effort was made to minimize the number of animals used and their suffering.

Antibodies

Rabbit polyclonal antibodies reactive to both human and mouse tau (pool-2) [45], specific to 4R tau (R2) [45], and reactive to both human and mouse Aβ (β001) [28] were prepared in our laboratory. The mouse monoclonal antibody to pSer396/Ser404-tau (PHF-1) was a kind gift from Dr. Peter Davies (Department of Pathology, Albert Einstein College of Medicine, Bronx, NY). Mouse monoclonal antibodies specific to human APP (6E10; Covance, Princeton, NJ), Aβ oligomers (11A1; IBL, Fujioka, Japan), human tau (tau12; Abcam, Cambridge, UK), 3R tau (RD3; Merck Millipore, Billerica, MA), 4R tau (RD4; Merck Millipore), pSer202/Thr205-tau (AT8; Thermo Scientific, Waltham, MA), synaptophysin (SVP-38; Sigma, St. Louis, MO), the mature neuron marker NeuN (Chemicon, Temecula, CA), and rabbit antibodies specific to the postsynaptic density protein PSD-95 (Cell Signaling Technology, Danvers, MA) and actin (Sigma) were purchased.

Western blot

Mouse brains ($n = 4$ for each group) were homogenized by sonication in 4 volumes of 50 mM Tris–HCl, pH 7.6, 150 mM NaCl (TBS) containing protease inhibitor cocktail (P8340; Sigma). The homogenates were subjected to SDS-PAGE with 7 % NuPage Tris–Acetate gels (Invitrogen, Carlsbad, CA) and transferred to PVDF membranes (Millipore). APP, tau, and actin were probed with 6E10, tau12, and anti-actin antibodies followed by HRP-labeled second antibodies and the chemiluminescent substrate Immobilon Western (Millipore). Signals were visualized and quantified using a LAS-3000 luminescent image analyzer (Fujifilm, Tokyo, Japan).

The homogenates ($n = 3$–4 for each group) were fractionated by three-step ultracentrifugation including TBS, *N*-lauroylsarcosinate (sarkosyl), and guanidine hydrochloride (GuHCl) extraction, as described previously [48]. The GuHCl-extracts were 400-fold diluted in TBS containing P8340 and concentrated into the initial volumes using Amicon Ultra 30 K filter devices (Millipore). The 30 K flow-through fractions were pooled for detection of low-n Aβ oligomers (see below). Phosphorylated tau in the TBS- and neutralized GuHCl-extracts was detected by Western blot with PHF-1 and AT8 antibodies. Aliquots of the TBS- and neutralized GuHCl-extracts were treated with 400 U/ml (approximately 80 U/mg protein) of calf intestinal alkaline phosphatase (New England Biolabs, Ipswich, MA) at 37 °C overnight, as described previously [48]. Dephosphorylated tau in the treated samples was probed with tau12, RD3 and RD4 antibodies.

For detection of Aβ oligomers higher than 30 kDa, the TBS- and neutralized GuHCl-extracts were applied onto 7 % Tris–Acetate gels, transferred to PVDF membranes, and stained with β001 antibody after the membranes were boiled in PBS for 10 min. To detect low-n Aβ oligomers, Aβ in the TBS-extracts and the 30 K flow-through fractions of GuHCl-extracts were immunoprecipitated with 6E10

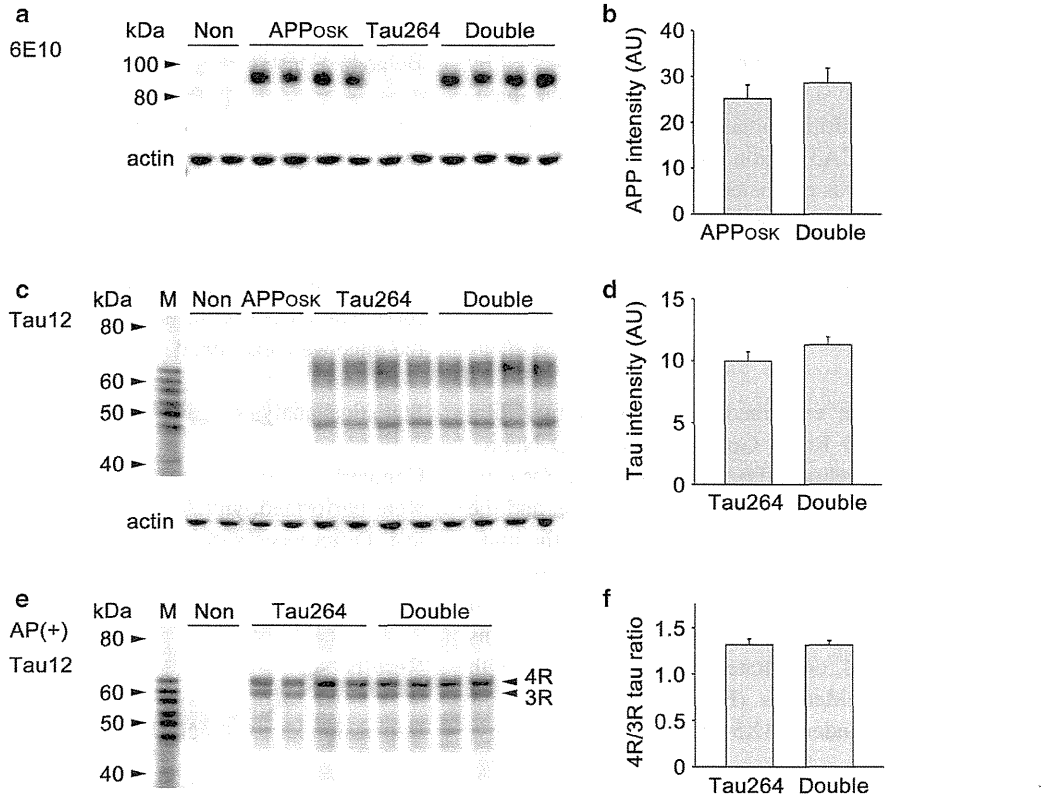

Fig. 1 Expression levels of human APP and tau in double Tg mice. **a** Brain homogenates from 6-month-old mice were subjected to Western blot with human APP-specific 6E10 antibody and anti-actin antibody. *Non* non-Tg mice, *Double* double Tg mice. **b** No significant difference in the expression level of human APP was observed between parent APP_{OSK}-Tg mice and double Tg mice. *AU* arbitrary unit. **c** Brain homogenates from 6-month-old mice were subjected to Western blot with human tau-specific tau12 antibody and anti-actin antibody. *M* recombinant human tau 6 isoforms. **d** No significant difference in the expression level of human tau was observed between parent tau264 mice and double Tg mice. **e** TBS-extracts from the brains of 6-month-old mice were treated with alkaline phosphatase (AP) and subjected to Western blot with tau12 antibody. **f** No significant difference in the ratio of 4R/3R tau was observed between parent tau264 mice and double Tg mice

antibody, applied onto 12 % NuPage Bis–Tris gels, and stained with β001 antibody after boiling the membranes.

Immunohistochemistry and Gallyas silver staining

Mice ($n = 4$–6 for each group) were perfused with 4 % paraformaldehyde, and the brains were removed, embedded in paraffin, and sectioned at 5 μm. Aβ accumulation and tau phosphorylation at 4, 6, 8, 12, 18, and 24 months, synapse loss at 6 and 12 months, and neuronal loss at 18 and 24 months were examined by immunohistochemistry, as described previously [46, 48]. Tangle formation was examined by Gallyas silver staining at 12, 18, and 24 months, as described previously [48]. The co-localization of 3R and 4R tau in cytoplasmic inclusions was examined at 24 months by double immunostaining with R2 and RD3 antibodies followed by FITC- and rhodamine-labeled second antibodies. Specimens were observed under a BX50 microscope (Olympus, Tokyo, Japan) and a Leica TCS SP5 confocal laser microscope (Leica, Wetzlar, Germany). Aβ oligomer accumulation was evaluated at 6 and 12 months by quantifying 11A1-positive areas in each photograph using NIH ImageJ software. Synapse loss was assessed by quantifying synaptophysin and PSD-95 fluorescence intensities in the apical dendritic-somata field (30 μm × 60 μm) of the hippocampal CA3 region using NIH ImageJ software. Neuronal loss was estimated by counting NeuN-positive cells in an area within 800 μm along the pyramidal cell layer of the hippocampal CA3 region and in an area of 1 × 1 mm in the retrosplenial region of the cerebral cortex.

Golgi staining

Dendritic spines were examined at 6 months by Golgi staining using the FD Rapid GolgiStain Kit (FD Neurotechnologies, Ellicott City, MD). Mice ($n = 1$–2 for each group) were perfused with 4 % paraformaldehyde, and the brains were removed and processed according to the manufacturer's instructions. After impregnation, brains were cut into 100 μm sections using a cryostat at −20 °C and mounted on gelatin-coated microscope slides. The sections were air-dried, stained, dehydrated, and coverslipped with Permount Mounting Medium (Fisher Scientific). Specimens were observed under a BX51 microscope (Olympus).

Immunoelectron microscopy

Tau filament formation was examined by post-embedding immunoelectron microscopy at 12, 18, and 24 months, as described previously [48]. Mouse brains ($n = 1$–2 for each group) were fixed in 4 % paraformaldehyde, 2.5 % glutaraldehyde, then 1 % osmium tetroxide, and embedded in epoxy resin. 70 nm-thick ultrathin sections were prepared and placed on H75-mesh carbon-coated copper grids. The sections were blocked with 5 % BSA/PBS and incubated with pool-2 antibody followed by 10 nm gold particle-labeled second antibody (AuroProbe EM GAR G10; Amersham). The specimens were then stained with 2.5 % lead citrate and 5 % uranyl acetate and viewed under an H-7500 electron microscope (Hitachi High-Technologies, Tokyo, Japan).

Fig. 2 Accelerated accumulation of intraneuronal Aβ oligomers in double Tg mice. **a** Brain sections were stained with Aβ oligomer-specific 11A1 antibody at various ages. APP_{OSK}-Tg mice exhibited intraneuronal accumulation of Aβ oligomers in the hippocampal CA3 region, cerebral cortex (CTX), and to a lesser extent the hippocampal CA1 region at 8 months. Double Tg mice displayed intraneuronal accumulation of Aβ oligomers in the CA3 region, cerebral cortex, and to a lesser extent the CA1 region at 6 months, which is earlier than parent APP_{OSK}-Tg mice. *Scale bar* 30 μm. **b** 11A1-positive areas in each photograph were quantified at 6 and 12 months using NIH ImageJ software. Data are given as mean ± SEM ($n = 5$ for non-Tg and APP_{OSK}-Tg at 6 months, $n = 4$ for tau264 and double Tg at 6 months, $n = 5$ for non-Tg, APP_{OSK}-Tg and tau264 at 12 months, $n = 4$ for double Tg at 12 months)

Behavioral tests

Spatial reference memory in mice was assessed at 6 months using the Morris water maze, essentially as described previously [46]. Male mice ($n = 5$–10 for each group) were trained to swim to a hidden platform for five consecutive days. Training consisted of five trials per day with intertrial intervals of 5 min, and the time required to reach the platform was measured in each trial. Locomotor activities of the mice were examined by an open-field test [46].

Statistical analysis

Comparisons of means among more than two groups were performed with ANOVA followed by Fisher's PLSD test. Differences with a p value of <0.05 were considered significant.

Results

Expression levels of human APP and tau in double Tg mice

To investigate the role of human tau in NFT formation, we crossbred APP_{OSK}-Tg mice with tau264 mice. The siblings were divided into four groups according to their genotype: non-Tg, APP_{OSK}-Tg, tau264, and double Tg, which express both APP_{OSK} and wild-type human tau. The levels of expression of APP and tau were examined by Western blot with human APP-specific 6E10 antibody and human tau-specific tau12 antibody at 6 months. No significant differences

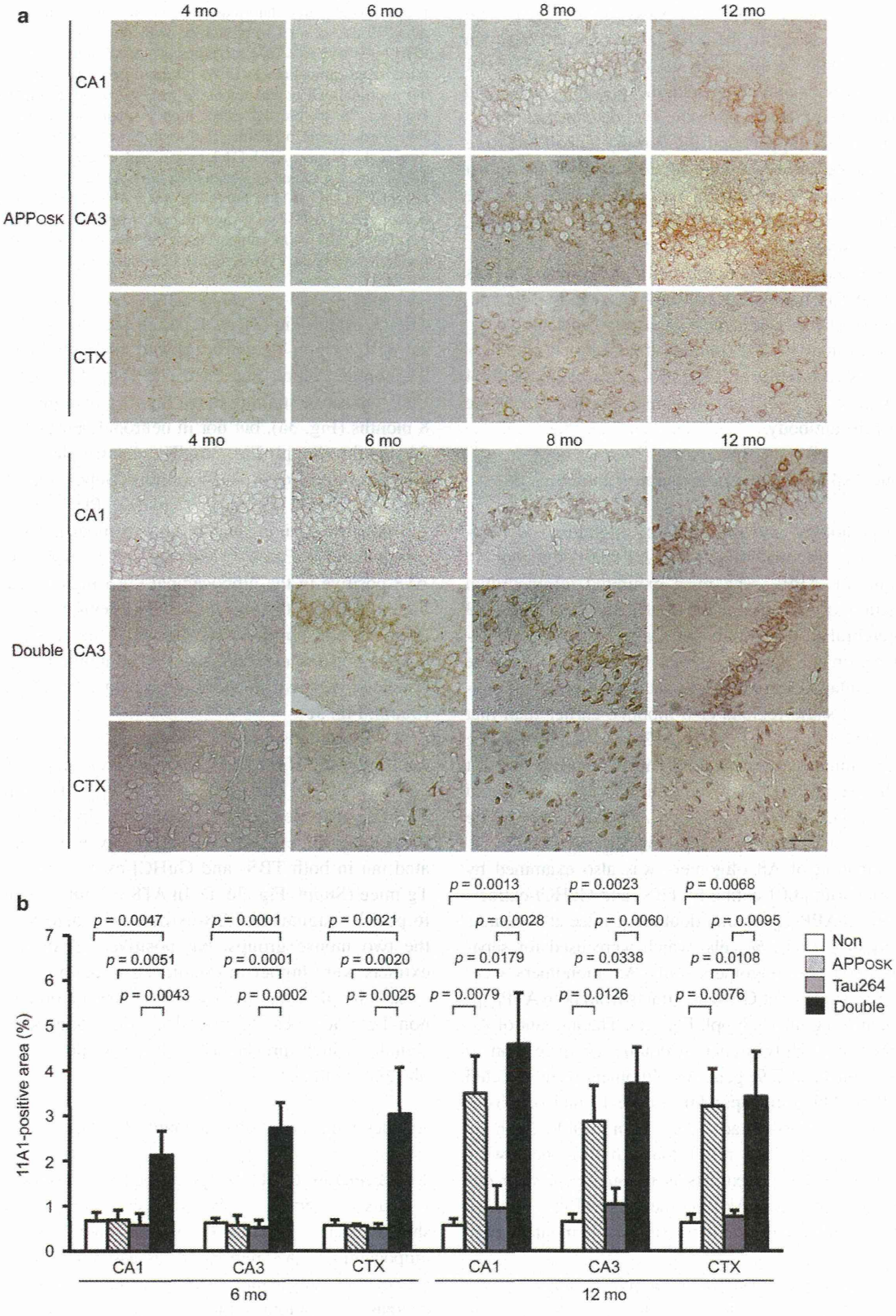
a
4 mo
6 mo
8 mo
12 mo
APPosk
Double
CA1
CA3
CTX
b
11A1-positive area (%)
Non
APPosk
Tau264
Double
p = 0.0047
p = 0.0051
p = 0.0043
p = 0.0001
p = 0.0001
p = 0.0002
p = 0.0021
p = 0.0020
p = 0.0025
p = 0.0013
p = 0.0028
p = 0.0079
p = 0.0023
p = 0.0060
p = 0.0126
p = 0.0068
p = 0.0095
p = 0.0108
p = 0.0076
6 mo
12 mo

were detected in APP expression between APP_{OSK}-Tg and double Tg mice (Fig. 1a, b) or in tau expression between tau264 and double Tg mice (Fig. 1c, d). The ratio of 3R/4R human tau was examined in alkaline phosphatase-treated TBS-extracts using tau12 antibody. Two discrete bands corresponding to 4R (upper) and 3R (lower) human tau were detected, and the ratio in double Tg mice was similar to that in the parent tau264 mice (Fig. 1e, f). However, while the lower bands were clearly stained with RD3 antibody (Suppl. Fig. 1a), the upper bands were not stained with RD4 antibody (Suppl. Fig. 1b). We confirmed that no mutation was incorporated into tau exon 10 of the transgene by sequencing genomic DNAs obtained from tau264 and double Tg mouse tails. It may be that some posttranslational modifications, such as acetylation at K280 [10], occurred in the RD4 epitope region (275–290 aa) of human tau to prevent the binding of the antibody.

Accelerated Aβ accumulation in double Tg mice

Amyloid pathology was examined by immunohistochemistry with Aβ oligomer-specific 11A1 antibody (Fig. 2, Suppl. Fig. 2). APP_{OSK}-Tg mice exhibited intraneuronal accumulation of Aβ oligomers in the hippocampal CA3 region, cerebral cortex, and to a lesser extent the hippocampal CA1 region at 8 months (Fig. 2a, b). In contrast, double Tg mice displayed intraneuronal accumulation of Aβ oligomers in the same regions at 6 months, earlier than that in the parent APP_{OSK}-Tg mice (Fig. 2a, b). Neither non-Tg nor tau264 mice showed 11A1-positive staining even at 24 months (Suppl. Fig. 2a). We confirmed that no amyloid plaque formation occurred in either APP_{OSK}-Tg or double Tg mice even at 24 months (Suppl. Fig. 2b).

The formation of Aβ oligomers was also examined by Western blot with β001 antibody. TBS- and GuHCl-extracts prepared from APP_{OSK}-Tg and double Tg mice at 6 months were compared. In 12 % gels, which were used for separation of low-n Aβ oligomers, only Aβ monomers were detected in TBS- but not GuHCl-extracts from both APP_{OSK}-Tg and double Tg mice (Suppl. Fig. 2c). The amount of Aβ monomers was slightly higher in double Tg mice than in APP_{OSK}-Tg mice. In 7 % gels, Aβ oligomers were detected around 50–60 kDa (corresponding to the 12-mer of Aβ) in GuHCl- but not TBS-extracts only from double Tg mice (Suppl. Fig. 2c, d). The result that Aβ oligomers were detected only in GuHCl-extracts is in agreement with our previous observation that Aβ oligomers in APP_{OSK}-Tg mice were detected in brain insoluble fractions at 24 months [46].

Accelerated tau phosphorylation in double Tg mice

Tau pathology was examined by immunohistochemistry with phosphorylated tau-specific PHF-1 and AT8 antibodies (Fig. 3, Suppl. Fig. 3). As reported previously [48], tau264 as well as non-Tg mice showed no pathology even at 24 months (Suppl. Fig. 3a–d). APP_{OSK}-Tg mice exhibited PHF-1-positive staining in the hippocampal mossy fibers at 8 months (Fig. 3a), but not in neuronal cell bodies even at 24 months (Suppl. Fig. 3c). These mice showed no AT8-positive signals even at 24 months (Suppl. Fig. 3b, d). In contrast, double Tg mice displayed PHF-1-positive and AT8-positive staining in the hippocampal mossy fibers at 6 months (Fig. 3a, b). Neuronal cell bodies also became AT8-positive in the hippocampal CA3 region and cerebral cortex at 6 months and in the CA1 regions at 12 months (Fig. 3b) and became PHF-1-positive in the hippocampal CA3 region and cerebral cortex at 12 months (Fig. 3a), but remained negative in the CA1 region even at 24 months (Suppl. Fig. 3c).

Fig. 3 Accelerated abnormal phosphorylation of tau in double Tg mice. Brain sections were stained with phosphorylated tau-specific PHF-1 (**a**) and AT8 (**b**) antibodies at various ages. **a** In APP_{OSK}-Tg mice, hippocampal mossy fibers became PHF-1-positive at 8 months, but neuronal cell bodies remained negative up to 24 months (Suppl. Fig. 3c). In double Tg mice, hippocampal mossy fibers became PHF-1-positive at 6 months, and neuronal cell bodies became positive in the hippocampal CA3 region and cerebral cortex (CTX) at 12 months, but remained negative in the CA1 region up to 24 months (Suppl. Fig. 3c). **b** In double Tg mice, hippocampal mossy fibers became AT8-positive at 6 months, and neuronal cell bodies became positive in the hippocampal CA3 region and cerebral cortex at 6 months and in the CA1 region at 12 months. *Scale bar* 30 μm

Tau hyperphosphorylation was also examined by Western blot with PHF-1 and AT8 antibodies. Again, TBS- and GuHCl-extracts prepared from APP_{OSK}-Tg and double Tg mice at 6 months were compared. In PHF-1 staining, double Tg mice exhibited higher levels of phosphorylated tau in both TBS- and GuHCl-extracts than APP_{OSK}-Tg mice (Suppl. Fig. 3e, f). In AT8 staining, no difference in positive signals in TBS-extracts was detected between the two mouse groups, but positive signals in GuHCl-extracts were higher in double Tg mice than APP_{OSK}-Tg mice (Suppl. Fig. 3g, h). TBS-extracts prepared from non-Tg mice also exhibited PHF-1- and AT8-positive signals, which presumably represent physiological tau phosphorylation.

Accelerated synapse loss in double Tg mice

An acceleration of the pathology in double Tg mice was also observed in the synapses. Our previous study showed that in APP_{OSK}-Tg mice, synaptic density in the hippocampal CA3 region, as assessed by immunostaining of the presynaptic marker synaptophysin, began to decrease at 8 months [46]. Thus, we compared synaptic density in the hippocampal CA3 region of the 4 groups at 6 and 12 months. At 6 months, no significant differences

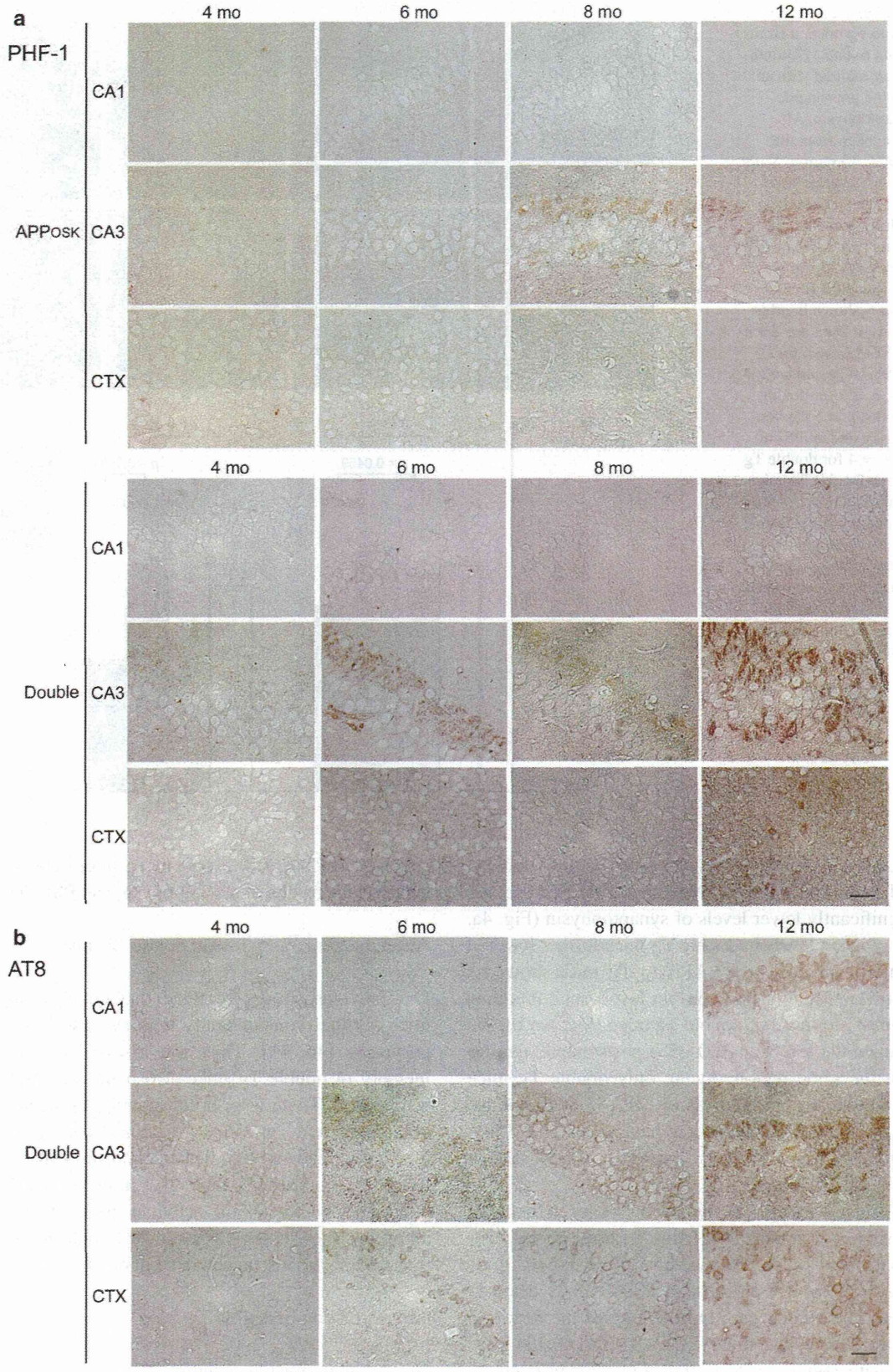
a
PHF-1
4 mo
6 mo
8 mo
12 mo
APPosK
CA1
CA3
CTX
Double
b
AT8

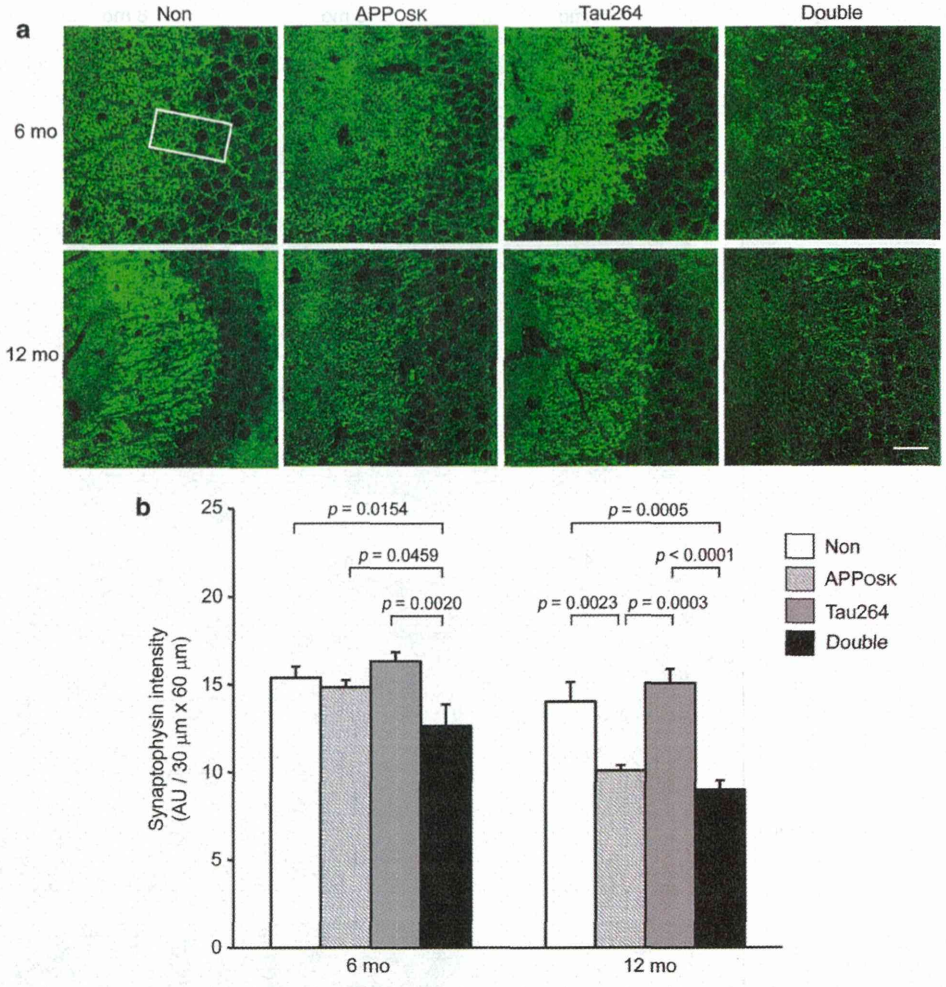

Fig. 4 Accelerated synapse loss in double Tg mice. **a** Brain sections from 6- and 12-month-old mice were stained with an antibody to the presynaptic marker synaptophysin. All images were taken from the hippocampal CA3 region. *Scale bar* 30 μm. **b** Synaptophysin fluorescence intensity in the apical dendritic-somata field (30 × 60 μm, rectangle) of the hippocampal CA3 region was quantified using NIH ImageJ software and is shown in arbitrary units (AU). Data are given as mean ± SEM ($n = 6$ for non-Tg, APP_{OSK}-Tg and tau264 at 6 months, $n = 5$ for double Tg at 6 months, $n = 5$ for non-Tg, APP_{OSK}-Tg and tau264 at 12 months, $n = 4$ for double Tg at 12 months). Double Tg mice displayed significantly lower levels of synaptophysin than the other groups at 6 months. By 12 months APP_{OSK}-Tg mice showed a significant decrease in synaptophysin levels such that they were similar to those of double Tg mice

in synaptophysin levels were observed among non-Tg, APP_{OSK}-Tg, and tau264 mice, whereas double Tg mice displayed significantly lower levels of synaptophysin (Fig. 4a, b). Synaptophysin levels in double Tg mice further lowered at 12 months, which is when APP_{OSK}-Tg mice showed a significant decrease in synaptophysin levels such that they became similar to those of double Tg mice (Fig. 4a, b). We also examined the levels of PSD-95, a postsynaptic density protein, in the same region. Again, only double Tg mice exhibited significant lower levels of PSD-95 at 6 months, and APP_{OSK}-Tg mice displayed a reduction in PSD-95 levels at 12 months to reach levels similar to those of double Tg mice (Suppl. Fig. 4a, b).

Synapse loss was also examined by Golgi staining of brain sections at 6 months. We focused on the apical dendritic-somata field of the hippocampal CA3 region, since the reduction of synaptophysin and PSD-95 was detected in this area. The number and morphology of the dendritic spines appeared unchanged in APP_{OSK}-Tg and tau264 mice compared with non-Tg mice (Suppl. Fig. 4c). In contrast, apparent loss and morphological alteration of dendritic spines were observed in double Tg mice. This observation supports the results of synaptophysin and PSD-95 stainings.

Accelerated memory loss in double Tg mice

Our previous studies revealed that cognitive function of mice declines concomitantly with synapse loss in the hippocampus [46, 48]. Thus, we assessed spatial reference memory of double Tg mice at 6 months using the Morris water maze. There were no differences in memory acquisition among non-Tg, APP_{OSK}-Tg, and tau264 mice, but double Tg mice showed significant deficits in performance, with longer escape latencies than other three groups (Fig. 5). No differences in locomotor activities were observed among all groups (not shown). These results indicate that memory impairment was also accelerated in double Tg mice.

NFT formation in double Tg mice

Our main interest is whether NFT formation occurs in the present double Tg mice, a pathology which has never

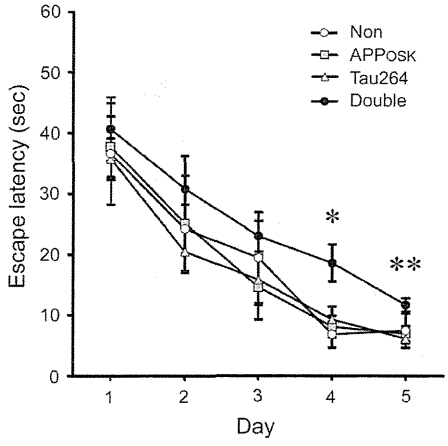

Fig. 5 Accelerated memory loss in double Tg mice. Spatial reference memory of mice was examined at 6 months using the Morris water maze. Male mice were trained to swim to a hidden platform for five consecutive days (five trials per day), and the time required to reach the platform was measured in each trial. Data are given as mean escape latency ± SEM ($n = 5$ for non-Tg, $n = 6$ for APP_{OSK}-Tg, $n = 10$ for tau264, $n = 8$ for double Tg). There were no differences in memory acquisition among non-Tg, APP_{OSK}-Tg, and tau264 mice, but double Tg mice showed significant deficits in performance, with longer escape latencies than the other three groups. *$p = 0.0051$ versus non-Tg, $p = 0.0080$ versus APP_{OSK}-Tg, $p = 0.0073$ versus tau263 at day 4; **$p = 0.0495$ versus non-Tg, $p = 0.0220$ versus APP_{OSK}-Tg, $p = 0.0032$ versus double Tg at day 5

been observed in APP-Tg mice including our APP_{OSK}-Tg mice. In Gallyas silver staining, double Tg mice displayed many positive signals within neurons in the hippocampal CA3 region and cerebral cortex, but not in the CA1 region, at 18 and 24 months (Fig. 6a). None of the other three groups showed positive signals even at 24 months (Suppl. Fig. 5a). To confirm the presence of tau filaments in the inclusions, immunoelectron microscopy with pool-2 anti-tau antibody was performed in double Tg mice. Tau-positive filamentous structures were abundantly observed within neurons in the hippocampal CA3 region and cerebral cortex at 18 and 24 months (Fig. 6b). The distribution of cytoplasmic PHF-1-positive and Gallyas-positive tau accumulation in double Tg mice paralleled that of the Aβ accumulation: dominant in the hippocampal CA3 region and cerebral cortex, and less so in the CA1 region. We noticed that this distribution was somewhat different from that of the tau pathology in our intronic mutant tau-Tg mice (lines 609 and 784), which have the same promoter and tau intronic sequences as tau264 mice: the mutant tau-Tg mice exhibited cytoplasmic PHF-1-positive and Gallyas-positive tau accumulation dominantly in the hippocampal CA1 region and cerebral cortex, and less so in the CA3 region [48]. This observation implies that NFT formation in double Tg mice was triggered by intracellular Aβ.

Whether the NFTs in double Tg mice contain both 3R and 4R tau is another issue of interest. Thus, we examined the co-localization of 3R and 4R tau at 24 months by immunohistochemistry with antibodies specific to these tau. While non-Tg and APP_{OSK}-Tg mice possessed only 4R tau, which should be endogenous mouse tau, both tau264 and double Tg mice expressed 3R tau, which presumably represents transgene-derived human tau, in addition to 4R tau (Fig. 6c, Suppl. Fig. 5b). In tau264 mice, both 3R and 4R tau were widely distributed in the hippocampal mossy fibers and neuronal cell bodies (Suppl. Fig. 5b). In contrast, double Tg mice exhibited less distribution of 4R tau in the mossy fibers and had 3R and 4R tau densely accumulate together in the neuronal cell bodies of the hippocampal CA3 region and cerebral cortex (Fig. 6c). This conclusion was confirmed by Western blot analysis for sarkosyl insoluble fractions (GuHCl-extracts) prepared from 18-month-old double Tg mice. Two discrete bands corresponding to 3R and 4R tau were detected with human tau-specific tau12 antibody after dephosphorylation of the samples (Suppl. Fig. 5c). These results indicate that the NFTs were comprised of both 3R and 4R human tau, which resembles the composition in AD.

Accelerated neuronal loss in double Tg mice

Neuronal loss, as well as senile plaques and NFTs, is a significant pathological feature of AD. In our previous study, APP_{OSK}-Tg mice displayed significant neuronal loss in the hippocampal CA3 region at 24 months, but not at 18 months or in the cerebral cortex even at 24 months [46]. Thus, we examined neuronal loss in the 4 groups at 12 and 18 months. The number of neurons positive for the mature neuron marker NeuN was counted in a constant area of the hippocampal CA3 region and cerebral cortex. In the CA3 region, no significant differences in number of NeuN-positive cells were measured among non-Tg, APP_{OSK}-Tg, and tau264 mice at 18 months, whereas double Tg mice possessed significantly fewer neurons than the other groups (Fig. 7a, b). No neuronal loss was observed at 12 months in either region (not shown) or in the cerebral cortex at 18 months (Fig. 7a, b) for all mice.

Discussion

In the present study, we generated double Tg mice expressing mutant APP and wild-type human tau to examine the role of human tau in NFT formations. While neither parent APP_{OSK}-Tg nor tau264 mice possessed NFTs even at 24 months, double Tg mice showed NFTs at 18 months. To our knowledge, the present double Tg mouse is the first mouse model of AD displaying not only Aβ accumulation,

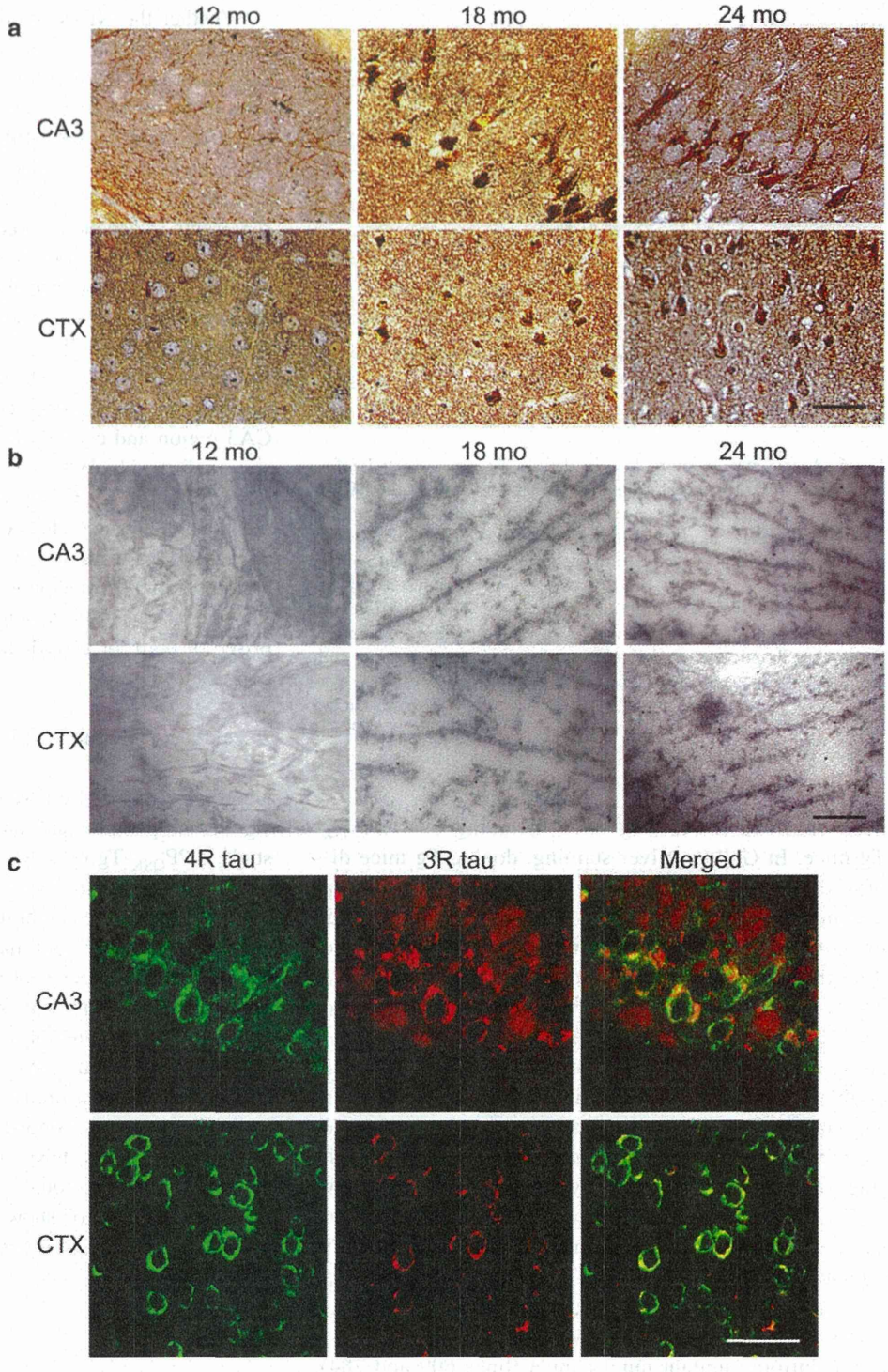

Fig. 6 NFT formation in double Tg mice. **a** Brain sections from double Tg mice were examined for NFTs by Gallyas silver staining at 12, 18, and 24 months. Many positive signals were detected at 18 and 24 months within neurons in the hippocampal CA3 region and cerebral cortex (CTX), but not the CA1 region (not shown). *Scale bar* 30 μm. **b** Brain ultrathin sections from double Tg mice were examined for tau filaments by immunoelectron microscopy with pool-2 anti-tau antibody and 10 nm gold particle-labeled second antibody at 12, 18, and 24 months. Tau-positive filamentous structures were abundantly observed within neurons in the hippocampal CA3 region and cerebral cortex at 18 and 24 months. *Scale bar* 200 nm. **c** Brain sections from 24-month-old double Tg mice were double stained with 3R tau-specific (*red*) and 4R tau-specific (*green*) antibodies. 3R and 4R tau were co-localized in neuronal cell bodies in the hippocampal CA3 region and cerebral cortex, and the distribution of 4R tau in the hippocampal mossy fibers was reduced compared with tau264 mice (Suppl. Fig. 5b). *Scale bar* 30 μm

but also NFT formation in the absence of tau mutations. It is noteworthy that these NFTs contained both 3R and 4R human tau, much like AD. This property makes the present Tg mice advantageous as a model for the investigation of the pathogenesis of AD. The distribution of cytoplasmic tau inclusions in double Tg mice paralleled Aβ accumulation, implying that NFT formation in these mice was triggered by intracellular Aβ. Our findings suggest that the presence of human tau, even at low levels (10 % of endogenous mouse tau), is critical for Aβ-induced NFT formation. Furthermore, the present Tg mice provide strong evidence that Aβ oligomers are the etiologic molecule in AD that causes

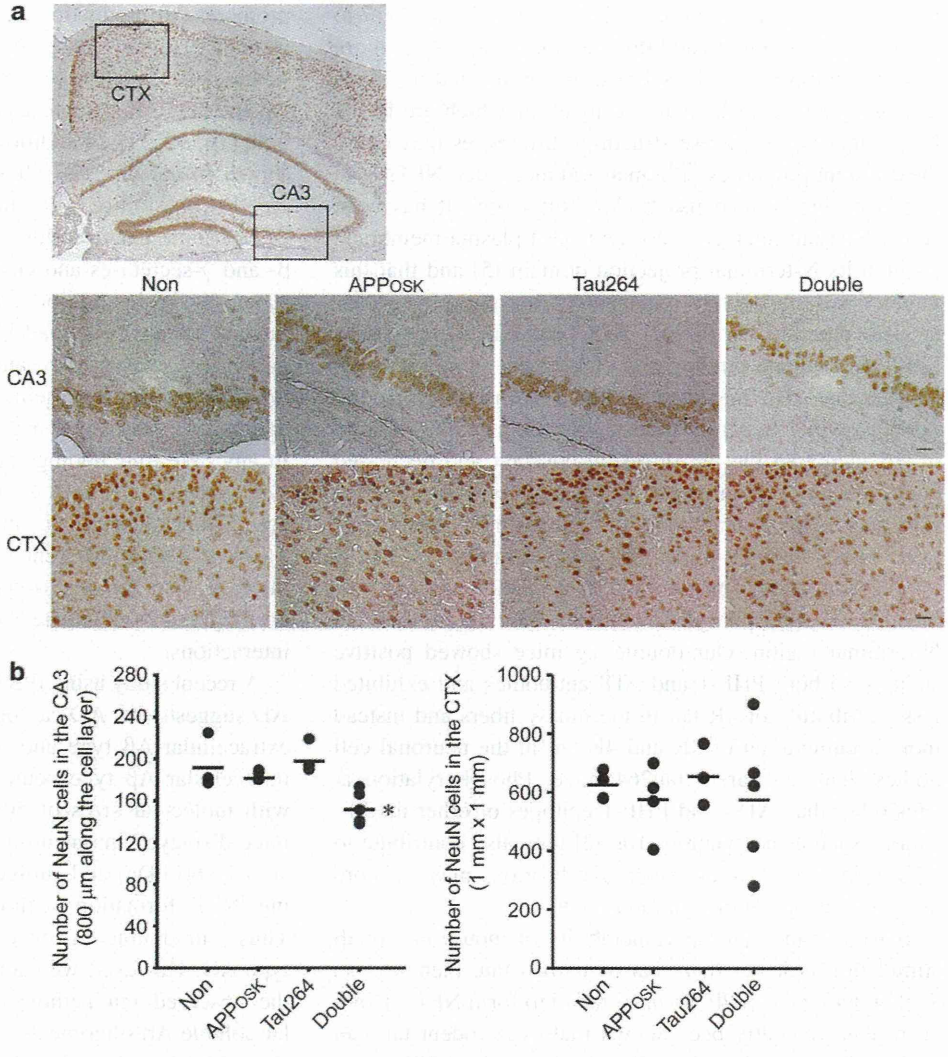

Fig. 7 Accelerated neuronal loss in double Tg mice. **a** Brain sections were stained with an antibody to the mature neuron marker NeuN at 12 and 18 months. Images of the hippocampal CA3 region (*lower rectangle* in the *top panel*) and retrosplenial region (*upper rectangle* in the *top panel*) of the cerebral cortex (CTX) at 18 months are shown. *Scale bar* 30 μm. **b** NeuN-positive cells in an area within 800 μm along the pyramidal cell layer in the hippocampal CA3 region and in an area of 1 × 1 mm in the retrosplenial region of the cerebral cortex were counted. *Dots* represent measured values for each mouse, and horizontal lines show mean values ($n = 3$ for Non-Tg and tau264, $n = 4$ for APP_{OSK}-Tg, $n = 5$ for double Tg). Double Tg mice possessed significantly fewer neurons in the hippocampus than the other groups at 18 months. $^*p = 0.0054$ versus Non-Tg, $p = 0.0175$ versus APP_{OSK}-Tg, $p = 0.0021$ versus tau264. No neuronal loss was observed at 12 months in either region (not shown) or in the cerebral cortex at 18 months for all mice

NFT formation as well as synapse and neuronal loss in the absence of amyloid plaques.

In vitro studies have shown no difference in aggregation tendency between human and mouse tau [7, 22]. Nevertheless, mouse tau appears to have a lower ability to form NFTs than human tau in vivo. Adams et al. [1] generated tau-Tg mice expressing wild-type mouse tau twofold endogenous levels by introducing the whole genome of mouse tau into the embryo. The mice developed age-dependent tau pathology, but did not show Gallyas-positive staining even at 18 months. On the other hand, Andorfer et al. [3] generated tau-Tg mice (htau mice) that express all six isoforms of wild-type human tau in the absence of endogenous mouse tau by mating genomic human tau-Tg mice (8c mice) with tau knockout mice. The expression levels of human tau in the parent 8c mice were more than threefold those of endogenous mouse tau. Despite the parent 8c mice not showing evident tau pathology, the htau mice developed intraneuronal accumulation of tau filaments at 9 months. These findings suggest that mouse tau hardly forms NFTs compared with human tau in vivo and that co-existence of mouse tau may interfere with the aggregation of human tau to prevent NFT formation. The latter hypothesis is supported by the finding that deletion of endogenous mouse tau accelerates the aggregation of human tau in mutant tau-Tg mice [2]. Therefore, NFT formation by human tau in the presence of mouse tau may require some driving forces such as tau mutations and Aβ stimulation unless human tau is massively overexpressed [19]. Once human tau starts to aggregate, it may act as a seed for the following aggregation of mouse tau. In fact, endogenous mouse tau has been shown before to aggregate together with human tau to form NFTs in mutant tau-Tg mice [33].

A noticeable difference between human and mouse tau exists in their N-terminal regions. Mouse tau lacks the 11

amino acids that correspond to the sequence from Thr17 to Gly27 in human tau. In addition, mouse tau possesses more than 30 amino acid substitutions, insertions, and deletions in comparison with human tau, many of which are in the N-terminal region. These structural differences may cause the different properties of human and mouse tau NFTs both in nature and in response to Aβ stimulation. It has been shown that tau interacts with the neural plasma membrane through its N-terminal projection domain [5] and that this interaction is negatively regulated by the phosphorylation at sites detected by PHF-1, AT8, and AT180 antibodies [29]. Microtubule binding and enrichment of tau at distal neurites are also mediated by the N-terminal projection domain, while hyperphosphorylation of tau and addition of Aβ increased the tau diffusion constant and decreased tau binding to microtubules, which may explain tau accumulation in the somatodendritic compartment of neurons [49]. These findings imply that the N-terminal region of tau plays an important role in NFT formation and that Aβ-induced tau phosphorylation affects the function of the N-terminal region. Our double Tg mice showed positive staining to both PHF-1 and AT8 antibodies and exhibited less distribution of 4R tau in the mossy fibers and instead more accumulation of 3R and 4R tau in the neuronal cell bodies than the parent tau264 mice. Phosphorylation at sites other than AT8- and PHF-1-epitopes or other modifications such as acetylation [10, 32] may also contribute to NFT formation. Overall, such modifications may be more likely in human tau than in mouse tau.

If we assume that the vulnerability of mouse tau to Aβ stimulation is lower than that of human tau, then we can explain why most APP-Tg mice failed to form NFTs. However, it has recently been shown that even rodent tau can form NFTs under certain conditions. Cohen et al. [9] generated a novel Tg rat model (TgF344-AD) expressing mutant APP and mutant presenilin 1 (PS1). Those rats expressed 2.6-fold higher human APP harboring the Swedish mutation than endogenous rat APP and 6.2-fold higher human PS1 harboring the exon 9 deletion than endogenous rat PS1, resulting in a dramatic increase in Aβ (particularly Aβ42) production. The rat further developed age-dependent amyloid and tau pathology and showed significant neuronal loss at 16 months. Notably, Gallyas-positive inclusions were detected in close proximity to the amyloid plaques at 16 months, although it is unclear whether these inclusions indeed contained tau filaments. Our APP_{OSK}-Tg mice expressed human APP at almost the same levels as endogenous mouse APP and failed to form NFTs. These findings suggest that extremely high levels of Aβ stimulation can drive endogenous rodent tau to NFT formation.

The present double Tg mice showed an accelerated accumulation of Aβ oligomers compared with parent APP_{OSK}-Tg mice. This suggests that the expression of human tau promotes Aβ production and/or aggregation or inhibits Aβ clearance. It may be that Aβ and human tau directly interact within cells. In vitro and in vivo studies have suggested that Aβ and tau form complexes that promote the aggregation of both [16, 30, 31]. In addition, the Aβ-tau complex has been shown to enhance tau phosphorylation by GSK-3β [16]. Another possibility is that human tau may affect the activities of some enzymes involved in Aβ production, such as β- and γ-secretases and GSK-3α, or Aβ degradation, such as neprilysin. In addition, co-expression of human tau with mutant Aβ may overload the capacity of cellular mechanisms (i.e., proteasomes, autophagosomes, and lysosomes) to clear misfolded proteins, leading to incomplete degradation and subsequent accumulation of both Aβ and tau. In any case, our findings suggest that Aβ and human tau synergistically interact to accelerate each other's pathology. Similar synergistic interactions have been shown in Tg mice among different amyloidogenic proteins, including Aβ, prion, tau, and α-synuclein [8, 34]. Further studies are required to elucidate the mechanism underlying these interactions.

A recent study using iPS cells derived from patients with AD suggests that AD can be classified into two categories: extracellular Aβ type and intracellular Aβ type [24]. The intracellular Aβ type neurons accumulated Aβ oligomers with molecular sizes of 50–60 kDa [24]. Our double Tg mice displayed intraneuronal accumulation of Aβ oligomers (50–60 kDa) and subsequent neuropathologies including NFT formation without forming amyloid plaques. Thus, our double Tg mice represent the intracellular Aβ type AD. However, we cannot exclude the possibility that the observed tau pathology was induced by extracellular soluble Aβ oligomers, which are more distributed than intracellular ones and, therefore, only negligibly detected by immunohistochemistry. In cultured primary neurons, exogenously added Aβ oligomers induced tau hyperphosphorylation and neurodegeneration [11, 21]. In addition, Aβ oligomer-induced synaptic alteration and neurodegeneration have been shown to be mediated by cell surface membrane receptors, such as NMDA receptors, and dendritic tau in vivo and in vitro [20, 25, 27, 43, 44]. These findings would argue that extracellular Aβ oligomers are the active species that lead to tau hyperphosphorylation and NFT formation. The extent extracellular Aβ oligomers contribute to the pathologies in our double Tg mice remains for further study.

It has been shown that human and mouse Aβ have different properties of aggregation due to their difference in amino acid sequence, with human Aβ being far more susceptible to aggregation [13]. Analogous to the possible interference between human and mouse tau, it is possible that the co-existence of mouse Aβ interferes with the aggregation of human Aβ to prevent plaque formation. This may

explain why wild-type APP-Tg mice seldom form amyloid plaques. It may be that amyloid plaque formation by human Aβ in the presence of mouse Aβ requires APP mutations to enhance Aβ production and/or aggregation and that deletion of endogenous mouse Aβ promotes plaque formation by human Aβ. If this hypothesis is true, double knockin mice expressing wild-type human APP and all six isoforms of wild-type human tau in the absence of both endogenous mouse APP and tau could display both amyloid plaques and NFTs under certain conditions, such as aging, metabolic syndromes, and stress. Such mice would be an ideal model for the investigation of the pathogenesis of sporadic AD.

Acknowledgments We thank Naomi Sakama, Reina Fujita, Maiko Mori, and Hideki Nakagawa for technical assistance, and Peter Karagiannis for reading the manuscript. This study was supported by the Grants-in-Aid for Scientific Research from the Ministry of Education, Culture, Sports, Science and Technology of Japan (no. 23110514, 24111562, 24659434, 25290018); by the Grants-in-Aid from the Ministry of Health, Labour, and Welfare, Japan; by the research funding for longevity sciences (23–39) from the National Center for Geriatrics and Gerontology, Japan; and in part by the Strategic Research Program for Brain Sciences, the Ministry of Education, Culture, Sports, Science and Technology of Japan.

Conflict of interest The authors declare that they have no conflict of interest.

References

1. Adams SJ, Crook RJ, Deture M, Randle SJ, Innes AE, Yu XZ, Lin WL, Dugger BN, McBride M, Hutton M, Dickson DW, McGowan E (2009) Overexpression of wild-type murine tau results in progressive tauopathy and neurodegeneration. Am J Pathol 175:1598–1609
2. Ando K, Leroy K, Héraud C, Yilmaz Z, Authelet M, Suain V, De Decker R, Brion JP (2011) Accelerated human mutant tau aggregation by knocking out murine tau in a transgenic mouse model. Am J Pathol 178:803–816
3. Andorfer C, Kress Y, Espinoza M, de Silva R, Tucker KL, Barde YA, Duff K, Davies P (2003) Hyperphosphorylation and aggregation of tau in mice expressing normal human tau isoforms. J Neurochem 86:582–590
4. Bolmont T, Clavaguera F, Meyer-Luehmann M, Herzig MC, Radde R, Staufenbiel M, Lewis J, Hutton M, Tolnay M, Jucker M (2007) Induction of tau pathology by intracerebral infusion of amyloid-β-containing brain extract and by amyloid-β deposition in APP × tau transgenic mice. Am J Pathol 171: 2012–2020
5. Brandt R, Léger J, Lee G (1995) Interaction of tau with the neural plasma membrane mediated by tau's amino-terminal projection domain. J Cell Biol 131:1327–1340
6. Chambers JK, Uchida K, Harada T, Tsuboi M, Sato M, Kubo M, Kawaguchi H, Miyoshi N, Tsujimoto H, Nakayama H (2012) Neurofibrillary tangles and the deposition of a beta amyloid peptide with a novel N-terminal epitope in the brains of wild Tsushima leopard cats. PLoS One 7:e46452
7. Chohan MO, Haque N, Alonso A, El-Akkad E, Grundke-Iqbal I, Grover A, Iqbal K (2005) Hyperphosphorylation-induced self assembly of murine tau: a comparison with human tau. J Neural Transm 112:1035–1047
8. Clinton LK, Blurton-Jones M, Myczek K, Trojanowski JQ, LaFerla FM (2010) Synergistic Interactions between Aβ, tau, and α-synuclein: acceleration of neuropathology and cognitive decline. J Neurosci 30:7281–7289
9. Cohen RM, Rezai-Zadeh K, Weitz TM, Rentsendorj A, Gate D, Spivak I, Bholat Y, Vasilevko V, Glabe CG, Breunig JJ, Rakic P, Davtyan H, Agadjanyan MG, Kepe V, Barrio JR, Bannykh S, Szekely CA, Pechnick RN, Town T (2013) A transgenic Alzheimer rat with plaques, tau pathology, behavioral impairment, oligomeric Aβ, and frank neuronal loss. J Neurosci 33:6245–6256
10. Cohen TJ, Guo JL, Hurtado DE, Kwong LK, Mills IP, Trojanowski JQ, Lee VM (2011) The acetylation of tau inhibits its function and promotes pathological tau aggregation. Nat Commun 2:252
11. De Felice FG, Wu D, Lambert MP, Fernandez SJ, Velasco PT, Lacor PN, Bigio EH, Jerecic J, Acton PJ, Shughrue PJ, Chen-Dodson E, Kinney GG, Klein WL (2008) Alzheimer's disease-type neuronal tau hyperphosphorylation induced by Aβ oligomers. Neurobiol Aging 29:1334–1347
12. Duyckaerts C, Potier MC, Delatour B (2008) Alzheimer disease models and human neuropathology: similarities and differences. Acta Neuropathol 115:5–38
13. Dyrks T, Dyrks E, Masters CL, Beyreuther K (1993) Amyloidogenicity of rodent and human βA4 sequences. FEBS Lett 324:231–236
14. Frank S, Clavaguera F, Tolnay M (2008) Tauopathy models and human neuropathology: similarities and differences. Acta Neuropathol 115:39–53
15. Goedert M, Spillantini MG, Cairns NJ, Crowther RA (1992) Tau proteins of Alzheimer paired helical filaments: abnormal phosphorylation of all six brain isoforms. Neuron 8:159–168
16. Guo JP, Arai T, Miklossy J, McGeer PL (2006) Aβ and tau form soluble complexes that may promote self aggregation of both into the insoluble forms observed in Alzheimer's disease. Proc Natl Acad Sci USA 103:1953–1958
17. Hardy J, Allsop D (1991) Amyloid deposition as the central event in the aetiology of Alzheimer's disease. Trends Pharmacol Sci 12:383–388
18. Hurtado DE, Molina-Porcel L, Iba M, Aboagye AK, Paul SM, Trojanowski JQ, Lee VM (2010) Aβ accelerates the spatiotemporal progression of tau pathology and augments tau amyloidosis in an Alzheimer mouse model. Am J Pathol 177:1977–1988
19. Ishihara T, Zhang B, Higuchi M, Yoshiyama Y, Trojanowski JQ, Lee VM (2001) Age-dependent induction of congophilic neurofibrillary tau inclusions in tau transgenic mice. Am J Pathol 158:555–562
20. Ittner LM, Ke YD, Delerue F, Bi M, Gladbach A, van Eersel J, Wölfing H, Chieng BC, Christie MJ, Napier IA, Eckert A, Staufenbiel M, Hardeman E, Götz J (2010) Dendritic function of tau mediates amyloid-β toxicity in Alzheimer's disease mouse models. Cell 142:387–397
21. Jin M, Shepardson N, Yang T, Chen G, Walsh D, Selkoe DJ (2011) Soluble amyloid β-protein dimers isolated from Alzheimer cortex directly induce tau hyperphosphorylation and neuritic degeneration. Proc Natl Acad Sci USA 108:5819–5824
22. Kampers T, Pangalos M, Geerts H, Wiech H, Mandelkow E (1999) Assembly of paired helical filaments from mouse tau: implications for the neurofibrillary pathology in transgenic mouse models for Alzheimer's disease. FEBS Lett 451:39–44
23. Klein WL (2013) Synaptotoxic amyloid-β oligomers: a molecular basis for the cause, diagnosis, and treatment of Alzheimer's disease? J Alzheimers Dis 33:S49–S65
24. Kondo T, Asai M, Tsukita K, Kutoku Y, Ohsawa Y, Sunada Y, Imamura K, Egawa N, Yahata N, Okita K, Takahashi K, Asaka I, Aoi T, Watanabe A, Watanabe K, Kadoya C, Nakano R, Watanabe D, Maruyama K, Hori O, Hibino S, Choshi T, Nakahata T, Hioki H, Kaneko T, Naitoh M, Yoshikawa K, Yamawaki S, Suzuki S,

Hata R, Ueno S, Seki T, Kobayashi K, Toda T, Murakami K, Irie K, Klein WL, Mori H, Asada T, Takahashi R, Iwata N, Yamanaka S, Inoue H (2013) Modeling Alzheimer's disease with iPSCs reveals stress phenotypes associated with intracellular Aβ and differential drug responsiveness. Cell Stem Cell 12:487–496
25. Lacor PN, Buniel MC, Furlow PW, Clemente AS, Velasco PT, Wood M, Viola KL, Klein WL (2007) Aβ oligomer-induced aberrations in synapse composition, shape, and density provide a molecular basis for loss of connectivity in Alzheimer's disease. J Neurosci 27:796–807
26. Lewis J, Dickson DW, Lin WL, Chisholm L, Corral A, Jones G, Yen SH, Sahara N, Skipper L, Yager D, Eckman C, Hardy J, Hutton M, McGowan E (2001) Enhanced neurofibrillary degeneration in transgenic mice expressing mutant tau and APP. Science 293:1487–1491
27. Li S, Hong S, Shepardson NE, Walsh DM, Shankar GM, Selkoe D (2009) Soluble oligomers of amyloid β protein facilitate hippocampal long-term depression by disrupting neuronal glutamate uptake. Neuron 62:788–801
28. Lippa CF, Ozawa K, Mann DM, Ishii K, Smith TW, Arawaka S, Mori H (1999) Deposition of β-amyloid subtypes 40 and 42 differentiates dementia with Lewy bodies from Alzheimer disease. Arch Neurol 56:1111–1118
29. Maas T, Eidenmüller J, Brandt R (2000) Interaction of tau with the neural membrane cortex is regulated by phosphorylation at sites that are modified in paired helical filaments. J Biol Chem 275:15733–15740
30. Manczak M, Reddy PH (2013) Abnormal interaction of oligomeric amyloid-β with phosphorylated tau: Implications to synaptic dysfunction and neuronal damage. J Alzheimers Dis 36:285–295
31. Miller Y, Ma B, Nussinov R (2011) Synergistic interactions between repeats in tau protein and Aβ amyloids may be responsible for accelerated aggregation via polymorphic states. Biochemistry 50:5172–5181
32. Min SW, Cho SH, Zhou Y, Schroeder S, Haroutunian V, Seeley WW, Huang EJ, Shen Y, Masliah E, Mukherjee C, Meyers D, Cole PA, Ott M, Gan L (2010) Acetylation of tau inhibits its degradation and contributes to tauopathy. Neuron 67:953–966
33. Mocanu MM, Nissen A, Eckermann K, Khlistunova I, Biernat J, Drexler D, Petrova O, Schönig K, Bujard H, Mandelkow E, Zhou L, Rune G, Mandelkow EM (2008) The potential for β-structure in the repeat domain of tau protein determines aggregation, synaptic decay, neuronal loss, and coassembly with endogenous tau in inducible mouse models of tauopathy. J Neurosci 28:737–748
34. Morales R, Estrada LD, Diaz-Espinoza R, Morales-Scheihing D, Jara MC, Castilla J, Soto C (2010) Molecular cross talk between misfolded proteins in animal models of Alzheimer's and prion diseases. J Neurosci 30:4528–4535
35. Oddo S, Caccamo A, Shepherd JD, Murphy MP, Golde TE, Kayed R, Metherate R, Mattson MP, Akbari Y, LaFerla FM (2003) Triple-transgenic model of Alzheimer's disease with plaques and tangles: intracellular Aβ and synaptic dysfunction. Neuron 39:409–421
36. Oikawa N, Kimura N, Yanagisawa K (2010) Alzheimer-type tau pathology in advanced aged nonhuman primate brains harboring substantial amyloid deposition. Brain Res 1315:137–149
37. Paulson JB, Ramsden M, Forster C, Sherman MA, McGowan E, Ashe KH (2008) Amyloid plaque and neurofibrillary tangle pathology in a regulatable mouse model of Alzheimer's disease. Am J Pathol 173:762–772
38. Ribé EM, Pérez M, Puig B, Gich I, Lim F, Cuadrado M, Sesma T, Catena S, Sánchez B, Nieto M, Gómez-Ramos P, Morán MA, Cabodevilla F, Samaranch L, Ortiz L, Pérez A, Ferrer I, Avila J, Gómez-Isla T (2005) Accelerated amyloid deposition, neurofibrillary degeneration and neuronal loss in double mutant APP/tau transgenic mice. Neurobiol Dis 20:814–822
39. Rosen RF, Farberg AS, Gearing M, Dooyema J, Long PM, Anderson DC, Davis-Turak J, Coppola G, Geschwind DH, Paré JF, Duong TQ, Hopkins WD, Preuss TM, Walker LC (2008) Tauopathy with paired helical filaments in an aged chimpanzee. J Comp Neurol 509:259–270
40. Schultz C, Dehghani F, Hubbard GB, Thal DR, Struckhoff G, Braak E, Braak H (2000) Filamentous tau pathology in nerve cells, astrocytes, and oligodendrocytes of aged baboons. J Neuropathol Exp Neurol 59:39–52
41. Seino Y, Kawarabayashi T, Wakasaya Y, Watanabe M, Takamura A, Yamamoto-Watanabe Y, Kurata T, Abe K, Ikeda M, Westaway D, Murakami T, Hyslop PS, Matsubara E, Shoji M (2010) Amyloid β accelerates phosphorylation of tau and neurofibrillary tangle formation in an amyloid precursor protein and tau double-transgenic mouse model. J Neurosci Res 88:3547–3554
42. Serizawa S, Chambers JK, Une Y (2012) Beta amyloid deposition and neurofibrillary tangles spontaneously occur in the brains of captive cheetahs (*Acinonyx jubatus*). Vet Pathol 49:304–312
43. Shankar GM, Bloodgood BL, Townsend M, Walsh DM, Selkoe DJ, Sabatini BL (2007) Natural oligomers of the Alzheimer amyloid-β protein induce reversible synapse loss by modulating an NMDA-type glutamate receptor-dependent signaling pathway. J Neurosci 27:2866–2875
44. Tackenberg C, Brandt R (2009) Divergent pathways mediate spine alterations and cell death induced by amyloid-β, wild-type tau, and R406W tau. J Neurosci 29:14439–14450
45. Takuma H, Arawaka S, Mori H (2003) Isoforms changes of tau protein during development in various species. Brain Res Dev Brain Res 142:121–127
46. Tomiyama T, Matsuyama S, Iso H, Umeda T, Takuma H, Ohnishi K, Ishibashi K, Teraoka R, Sakama N, Yamashita T, Nishitsuji K, Ito K, Shimada H, Lambert MP, Klein WL, Mori H (2010) A mouse model of amyloid β oligomers: their contribution to synaptic alteration, abnormal tau phosphorylation, glial activation, and neuronal loss in vivo. J Neurosci 30:4845–4856
47. Tomiyama T, Nagata T, Shimada H, Teraoka R, Fukushima A, Kanemitsu H, Takuma H, Kuwano R, Imagawa M, Ataka S, Wada Y, Yoshioka E, Nishizaki T, Watanabe Y, Mori H (2008) A new amyloid β variant favoring oligomerization in Alzheimer's-type dementia. Ann Neurol 63:377–387
48. Umeda T, Yamashita T, Kimura T, Ohnishi K, Takuma H, Ozeki T, Takashima A, Tomiyama T, Mori H (2013) Neurodegenerative disorder FTDP-17-related tau intron 10 +16C → T mutation increases tau exon 10 splicing and causes tauopathy in transgenic mice. Am J Pathol 183:211–225
49. Weissmann C, Reyher HJ, Gauthier A, Steinhoff HJ, Junge W, Brandt R (2009) Microtubule binding and trapping at the tip of neurites regulate tau motion in living neurons. Traffic 10:1655–1668

Cell Stem Cell
Short Article

Modeling Alzheimer's Disease with iPSCs Reveals Stress Phenotypes Associated with Intracellular Aβ and Differential Drug Responsiveness

Takayuki Kondo,[1,2,7] Masashi Asai,[7,9,10] Kayoko Tsukita,[1,7] Yumiko Kutoku,[11] Yutaka Ohsawa,[11] Yoshihide Sunada,[11] Keiko Imamura,[1] Naohiro Egawa,[1] Naoki Yahata,[1,7] Keisuke Okita,[1] Kazutoshi Takahashi,[1] Isao Asaka,[1] Takashi Aoi,[1] Akira Watanabe,[1] Kaori Watanabe,[7,10] Chie Kadoya,[7,10] Rie Nakano,[7,10] Dai Watanabe,[3] Kei Maruyama,[9] Osamu Hori,[12] Satoshi Hibino,[13] Tominari Choshi,[13] Tatsutoshi Nakahata,[1] Hiroyuki Hioki,[4] Takeshi Kaneko,[4] Motoko Naitoh,[5] Katsuhiro Yoshikawa,[5] Satoko Yamawaki,[5] Shigehiko Suzuki,[5] Ryuji Hata,[14] Shu-ichi Ueno,[15] Tsuneyoshi Seki,[16] Kazuhiro Kobayashi,[16] Tatsushi Toda,[16] Kazuma Murakami,[6] Kazuhiro Irie,[6] William L. Klein,[17] Hiroshi Mori,[18] Takashi Asada,[19] Ryosuke Takahashi,[2] Nobuhisa Iwata,[7,10,*] Shinya Yamanaka,[1,8] and Haruhisa Inoue[1,7,8,*]
[1]Center for iPS Cell Research and Application (CiRA)
[2]Department of Neurology, Graduate School of Medicine
[3]Department of Biological Sciences, Graduate School of Medicine and Department of Molecular and Systems Biology, Graduate School of Biostudies
[4]Department of Morphological Brain Science, Graduate School of Medicine
[5]Department of Plastic and Reconstructive Surgery, Graduate School of Medicine
[6]Organic Chemistry in Life Science, Division of Food Science and Biotechnology, Graduate School of Agriculture
Kyoto University, Kyoto 606-8507, Japan
[7]Core Research for Evolutional Science and Technology (CREST)
[8]Yamanaka iPS Cell Special Project
Japan Science and Technology Agency (JST), Saitama 332-0012, Japan
[9]Department of Pharmacology, Faculty of Medicine, Saitama Medical University, Saitama 350-0495, Japan
[10]Laboratory of Molecular Biology and Biotechnology, Department of Molecular Medicinal Sciences, Graduate School of Biomedical Sciences, Nagasaki University, Nagasaki 852-8521, Japan
[11]Department of Neurology, Kawasaki Medical School, Okayama 701-0192, Japan
[12]Department of Neuroanatomy (Biotargeting), Kanazawa University Graduate School of Medical Sciences, Ishikawa 920-8640, Japan
[13]Faculty of Pharmacy and Pharmaceutical Sciences, Fukuyama University, Hiroshima 729–0292, Japan
[14]Department of Functional Histology
[15]Department of Psychiatry
Ehime University Graduate School of Medicine, Ehime 791-0295, Japan
[16]Division of Neurology/Molecular Brain Science, Kobe University Graduate School of Medicine, Kobe, Hyogo 650-0017, Japan
[17]Department of Neurobiology, Northwestern University, Evanston, IL 60208, USA
[18]Department of Neuroscience, Graduate School of Medicine, Osaka City University, Osaka 545-8585, Japan
[19]Department of Neuropsychiatry, Institute of Clinical Medicine, University of Tsukuba, Ibaraki 305-8577, Japan
*Correspondence: haruhisa@cira.kyoto-u.ac.jp (H.I.), iwata-n@nagasaki-u.ac.jp (N.I.)
http://dx.doi.org/10.1016/j.stem.2013.01.009

SUMMARY

Oligomeric forms of amyloid-β peptide (Aβ) are thought to play a pivotal role in the pathogenesis of Alzheimer's disease (AD), but the mechanism involved is still unclear. Here, we generated induced pluripotent stem cells (iPSCs) from familial and sporadic AD patients and differentiated them into neural cells. Aβ oligomers accumulated in iPSC-derived neurons and astrocytes in cells from patients with a familial amyloid precursor protein (APP)-E693Δ mutation and sporadic AD, leading to endoplasmic reticulum (ER) and oxidative stress. The accumulated Aβ oligomers were not proteolytically resistant, and docosahexaenoic acid (DHA) treatment alleviated the stress responses in the AD neural cells. Differential manifestation of ER stress and DHA responsiveness may help explain variable clinical results obtained with the use of DHA treatment and suggests that DHA may in fact be effective for a subset of patients. It also illustrates how patient-specific iPSCs can be useful for analyzing AD pathogenesis and evaluating drugs.

INTRODUCTION

Alzheimer's disease (AD) is the most prevalent neurodegenerative disorder. One of the pathological features of AD is the oligomerization and aggregation and accumulation of amyloid-β peptide (Aβ), forming amyloid plaques in the brain. Cognitive impairment observed in clinical AD is inversely well correlated with the amount of Aβ oligomers in the soluble fraction rather than the amount of Aβ fibrils (amyloid plaques) constituting the oligomers (Haass and Selkoe, 2007; Krafft and Klein, 2010). Increasing evidence has shown that Aβ oligomers extracted from AD model mice or made from synthetic peptides cause

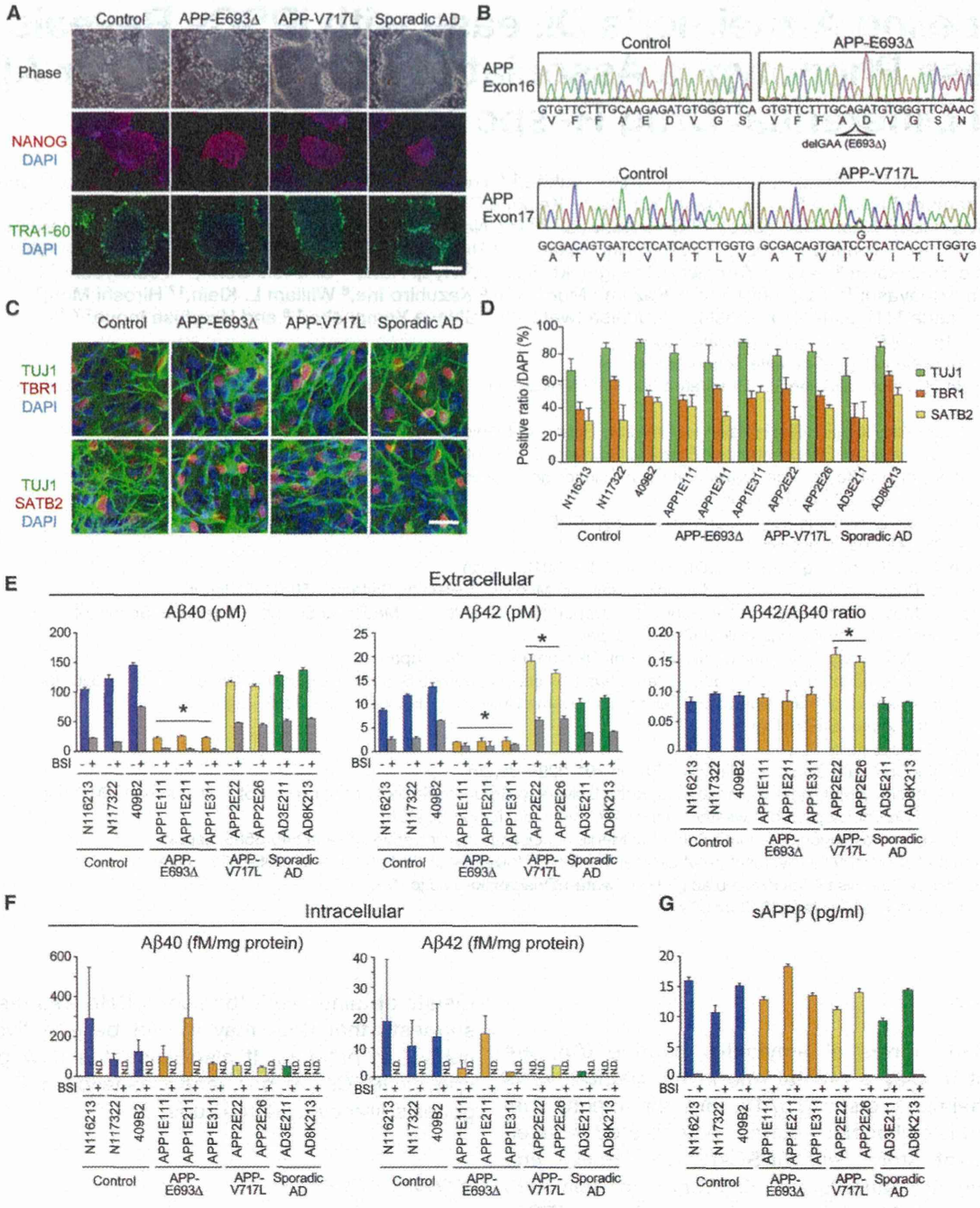

Figure 1. Establishment of Control and AD Patient-Specific iPSCs, and Derivation of Cortical Neurons Producing Aβs from iPSCs

(A) Established iPSCs from both controls and AD patients showed embryonic stem cell-like morphology (Phase) and expressed pluripotent stem cell markers NANOG (*red*) and TRA1-60 (*green*). *The scale bar represents 200 μm.*

(B) Genomic DNA sequences showed the presence of the homozygous genotype for E693 deletion and the heterozygous genotype for V717L mutation on the *APP* gene only in AD iPSCs.

(C) Estimation of neuronal differentiation from control and AD-iPSCs. After 2 months of differentiation, neurons were immunostained with antibodies against the neuronal marker TUJ1 and the cortical neuron markers TBR1 and SATB2. *The scale bar represents 30 μm.*

(D) Proportions of TUJ1-, TBR1-, and SATB2-positive cells in control and AD-iPSCs. Data represent mean ± SD (n = 3 per clone).

(E) Aβ40 and Aβ42 secreted from iPSC-derived neural cells into the medium (extracellular Aβ) were measured at 48 hr after the last medium change. Data represent mean ± SD (n = 3 per clone). Levels of Aβ40 and Aβ42 in AD(APP-E693Δ) without β-secretase inhibitor IV (BSI, 1 μM) were significantly lower than those of the others (*, $p < 0.006$), and the level of Aβ42 and the ratio of Aβ42/Aβ40 in AD(APP-V717L) without BSI were significantly higher than those of the others

(legend continued on next page)